



HAL
open science

Ki-67 and MCM6 labelling indices are correlated with overall survival in anaplastic oligodendroglioma, IDH1-mutant and 1p/19q-codeleted: a multicenter study from the French POLA network

Celso Pouget, Sébastien Hergalant, Emilie Lardenois, Stéphanie Lacomme, Rémi Houlgatte, Catherine Carpentier, Caroline Dehais, Fabien Rech, Luc Taillandier, Marc Sanson, et al.

► **To cite this version:**

Celso Pouget, Sébastien Hergalant, Emilie Lardenois, Stéphanie Lacomme, Rémi Houlgatte, et al.. Ki-67 and MCM6 labelling indices are correlated with overall survival in anaplastic oligodendroglioma, IDH1 -mutant and 1p/19q-codeleted: a multicenter study from the French POLA network. *Brain Pathology*, 2020, 30 (3), pp.465-478. 10.1111/bpa.12788 . hal-02299833

HAL Id: hal-02299833

<https://hal.univ-lorraine.fr/hal-02299833v1>

Submitted on 20 Sep 2023

HAL is a multi-disciplinary open access archive for the deposit and dissemination of scientific research documents, whether they are published or not. The documents may come from teaching and research institutions in France or abroad, or from public or private research centers.



L'archive ouverte pluridisciplinaire **HAL**, est destinée au dépôt et à la diffusion de documents scientifiques de niveau recherche, publiés ou non, émanant des établissements d'enseignement et de recherche français ou étrangers, des laboratoires publics ou privés.



Distributed under a Creative Commons Attribution 4.0 International License

RESEARCH ARTICLE

Ki-67 and MCM6 labeling indices are correlated with overall survival in anaplastic oligodendroglioma, *IDH1*-mutant and 1p/19q-codeleted: a multicenter study from the French POLA network

Celso Pouget^{1,2,*}; Sébastien Hergalant^{2,*} ; Emilie Lardenois^{1,2}; Stéphanie Lacomme³; Rémi Houlgatte²; Catherine Carpentier⁴; Caroline Dehais⁵; Fabien Rech^{6,7}; Luc Taillandier⁸; Marc Sanson^{4,5,9}; Romain Appay^{10,11}; Carole Colin¹⁰; Dominique Figarella-Branger^{10,11}; Shyue-Fang Battaglia-Hsu²; Guillaume Gauchotte^{1,2,3,*}  Investigators: The POLA Network

¹ Department of Pathology, CHRU, Nancy, France.

² INSERM U1256, NGERE, Faculté de Médecine de Nancy, Université de Lorraine, Vandoeuvre-lès-Nancy, France.

³ Centre de Ressources Biologiques, CHRU, BB-0033-00035, Nancy, France.

⁴ Sorbonne Universités, UPMC Univ Paris 06 UMR S 1127, Inserm U 1127, CNRS UMR 7225, ICM, F-75013, Paris, France.

⁵ AP-HP, Groupe Hospitalier Pitié-Salpêtrière, Service de Neurologie 2-Mazarin, 75013, Paris, France.

⁶ Department of Neurosurgery, CHRU, Nancy, France.

⁷ Institut des Neurosciences, INSERM U1051, Montpellier, France.

⁸ Department of Neurology, CHRU, Nancy, France.

⁹ Onconeurotek, Groupe Hospitalier Pitié-Salpêtrière, Paris, France.

¹⁰ Aix-Marseille Univ, CNRS, INP, Inst. Neurophysiopathol, Marseille, France.

¹¹ AP-HM, Hôpital de la Timone, Service d'Anatomie Pathologique et de Neuropathologie and Centre de Ressources Biologiques CRB-TBM, BB-0033-00097, Marseille, France.

Keywords

1p/19q codeletion, anaplastic oligodendroglioma, glioma, immune response, immunohistochemistry, Ki-67, MCM6, proliferation, pro-neural, transcriptomics.

Corresponding author:

Guillaume Gauchotte, MD, PhD, Service d'Anatomie et Cytologie Pathologiques, Hôpital Central, CHRU de Nancy, 29, avenue du Maréchal De Lattre de Tassigny, Nancy 54000, France
(E-mail: g.gauchotte@chru-nancy.fr)

Received 23 May 2019

Accepted 19 September 2019

Published Online Article Accepted

27 September 2019

*These two authors have contributed equally to this work.

doi:10.1111/bpa.12788

Abstract

Anaplastic oligodendroglioma (AO), *IDH*-mutant and 1p/19q codeleted (*IDH*mut+/1p19qcodelet), is a high-grade glioma with only limited prognostic markers. The primary objective of this study was to evaluate, by immunohistochemistry, the prognostic value of two proliferation markers, MCM6 and Ki-67, in a large series of *IDH*mut+/1p19qcodelet AO included in the POLA (“Prise en charge des Oligodendrogliomes Anaplasiques”) French national multicenter network. We additionally examined the transcriptome obtained from this series to understand the functional pathways dysregulated with the mRNA overexpression of these two markers. The labeling indices (LI) of MCM6 and Ki-67 were obtained via computer-assisted color image analyses on immunostained AO tissues of the cohort (n = 220). Furthermore, a subgroup of AO (n = 68/220) was used to perform transcriptomic analyses. A high LI of either MCM6 (≥50%) or Ki-67 (≥15%) correlated with shorter overall survival, both in univariate ($P = 0.013$ and $P = 0.004$, respectively) and multivariate analyses ($P = 0.027$; multivariate Cox model including age, mitotic index, MCM6 and Ki-67). MCM6 and Ki-67 LI also correlated with overall survival in an additional retrospective cohort of 30 grade II *IDH*mut+/1p19qcodelet oligodendrogliomas. The prognostic value of *MCM6* mRNA level was confirmed in The Cancer Genome Atlas (TCGA) *IDH*mut+/1p19qcodelet gliomas. The transcriptomic approach revealed that high transcriptional expressions of *MCM6* and *MKI67* were both linked positively with cell cycle progression, DNA replication, mitosis, pro-neural phenotype as well as neurogenesis, and negatively with microglial cell activation, immune response, positive regulation of myelination, oligodendrocyte development, beta-amyloid binding and postsynaptic specialization. In conclusion, the overexpression of MCM6 and/or Ki-67 is independently associated to shorter overall survival in *IDH*mut+/1p19qcodelet AO. These two easy-to-use and cost-effective markers could thus be used concurrently in routine pathology practice. Additionally, the transcriptomic analyses showed that AO with high proliferation index have down-regulated immune response and lower microglial cells activation, and bears pro-neural phenotype.

INTRODUCTION

According to the World Health Organization (WHO), *IDH*-mutant and 1p/19q-codeleted (*IDH*mut+/1p19qcodelet) anaplastic oligodendrogliomas (AOs) are high-grade gliomas, corresponding histologically to WHO grade III primary brain tumors (35). AO are rare, accounting for 0.5% of all primary brain tumors and one-third of oligodendroglial tumors (38). They are histologically defined as tumors of the oligodendroglial cells, with features of anaplasia, including increased cellularity and mitotic activity, microvascular proliferation and/or necrosis. Although Ki-67 labeling index (LI) is usually used to help differentiate low-grade from high-grade oligodendroglioma, no clear cut-off point has been established (12). By definition, and according to the 2016 update of the WHO Classification of Central Nervous System, AO carry both *IDH1/2* mutations and 1p/19q codeletion (10, 43). The standard of care for these tumors includes surgical resection in conjunction with adjuvant therapies like combined adjuvant radiochemotherapy with procarbazine, CCNU (lomustine), and vincristine (RT-PCV) to improve the overall survival (OS) (46).

The prognostic role of the WHO grading in *IDH*-mutant gliomas remains debatable, and this is particularly true in the case of oligodendrogliomas (43). In AO patients, young age, high Karnofsky index/clinical performance status, complete surgical resection and adjuvant therapy such as RT-PCV have been shown to associate with longer OS (45, 46). Histological features such as microvascular proliferation, mitotic index (MI) and necrosis have been found associated with three distinct prognostic subgroups of *IDH*-mut+/1p19qcodelet AO with other genomic alterations (19). These include mutations of *CIC* and *TCF12*, both linked to more aggressive AO (4, 22, 32), and allelic loss of 9p21.3, associated with shorter progression-free survival (PFS) and shorter OS in *IDH*-mut+/1p19qcodelet AO (2). Omics approaches using transcriptome, genome and methylome have also been used to identify potential prognostic factors. One such study has successfully classified oligodendroglial tumors into three molecular subgroups with distinct clinical behaviors (29). Machine learning algorithms aiming to identify copy number variations have also been applied recently to AO samples; such technique seems promising in helping with prognostic stratification (41). Despite of these advances, however, it is worth noting that all the above-mentioned markers of AO need expansive and time-consuming molecular analyses, and thus cannot be widely applied to all samples in all laboratories.

In contrast, immunohistochemical proliferation markers such as Ki-67, whose LI correlates strongly with prognosis of many tumor types, are simple, effective and economical means to assess tumor aggressivity. In the case of AO, past few evidence obtained using univariate—but not multivariate—analysis appeared to support the prognostic value of Ki-67 LI (40). However, as less than 50% of the AO tissues in this latter study (performed prior to the 2016 revision of the WHO classification) actually harbored *IDH* mutations and 1p/19q codeletion, its validity shall be questioned. In a more recent study, Zeng *et al* evaluated the prognostic

value of Ki-67 upon classifying gliomas into subgroups with either the presence or the absence of *IDH1/2*; however, data concerning 1p/19q values codeletion were lacking in the studied gliomas (49).

Several proliferation markers other than Ki-67 have also been studied in brain tumors. Notably, we previously reported that Minichromosome Maintenance Complex component 6 (MCM6) was overexpressed in meningioma, and was associated with higher histological grade and risk of recurrence (21). In adamantinomatous craniopharyngiomas, MCM6 correlated with a higher risk of long-term recurrence (48). In gliomas, especially in glioblastomas of the Chinese Cancer Genome Atlas (CCGA), *MCM6* mRNA overexpression was also reported to be correlated with poor overall survival (9).

Minichromosome Maintenance proteins (MCMs) play a key role in DNA synthesis and replication, forming a hexameric helicase complex around the DNA (31). All MCMs (MCM2-7) are detectable during the different phases of the cell cycle, including G1, S, G2 and M, but are absent in G0 (33). These proteins are also expressed earlier during G1, in comparison with Ki-67. In other solid tumors, like non-small cell lung carcinomas (47), hepatocellular carcinomas (34), endometrial carcinomas (26), low-grade chondrosarcomas (24) and mantle cell lymphomas (42), a high MCM6 LI correlated with a worse prognosis. To our knowledge since the revision of the 4th WHO classification of 2016, MCMs, and notably MCM6, have never been specifically studied in *IDH*mut+/1p19qcodelet AO.

The primary goal of this study was therefore to evaluate and compare, by immunohistochemistry, the prognostic value of MCM6 and Ki-67 in a large series of *IDH*mut+/1p19qcodelet AO obtained from the POLA (“Prise en charge des Oligodendrogliomes Anaplasiques”) French national multicenter network. We additionally examined the transcriptomes obtained from part of this series to understand the functional pathways dysregulated with the mRNA overexpression of these two markers.

MATERIAL AND METHODS

Population and clinicopathological data

Two hundred and thirty-one cases of *IDH*mut+/1p19qcodelet AO were retrieved from the French national multicenter POLA cohort. Clinical data, such as age, sex, extent of surgical removal, type of adjuvant treatment and OS are available in the database, as well as molecular data, including *IDH* mutation status and presence of 1p/19q codeletion. All cases included in this cohort have been centrally reviewed by the neuropathologists of the national board of French national POLA network and were classified according to the 2016 4th WHO classification update. The MI and Ki-67 LI were evaluated in whole tissue sections, as previously described (18). In 220 out of 231 patients, tissue microarray (TMA) blocks were designed with representative samples of tumors, in order to perform immunohistochemical analyses. One to three spots were available for each case.

Additionally, in order to evaluate the prognostic value of MCM6 and Ki-67 LI in low-grade tumors, 30 cases of grade II IDHmut+/1p19qcode1 oligodendrogliomas (IDHmut+/1p19qcode1 OII) were retrieved from the files of the Department of Neuropathology at Pitié-Salpêtrière Hospital (AP-HP, Paris; OncoNeuroTek database; Pitié-Salpêtrière) and the Department of Pathology at Nancy University Hospital (CHRU, Nancy; Centre de Ressources Biologiques, BB-0033-00035).

Ethics

Anonymity was strictly respected, according to the principles of the declaration of Helsinki and national ethical guidelines. Patients consent for clinical data collection and genetic analyses have been obtained prospectively, according to POLA network policies. The study was approved by the ethics committee of Hôpital Universitaire la Pitié-Salpêtrière.

Immunohistochemistry

Paraffin sections of 5 µm thickness were immersed in a 10mM sodium citrate buffer (pH 6) for 20 minutes at 97°C for dewaxing and antigen retrieval. The following primary antibodies were used: MCM6 (1/400; goat polyclonal, Santa Cruz Biotechnology, Heidelberg, Germany), Ki-67 (1/200; mouse monoclonal, MIB-1, Dako Cytomation, Glostrup, Denmark).

Immunohistochemistry was performed with Dako Autostainer Plus (Dako) and the Flex + Envision revelation system (Dako).

Ki-67 and MCM6 evaluation

Ki-67 and MCM6 labeling indices (LI) were defined as the percentage of cells with positive nuclear stain of the two individual markers, independently from the signal intensity. For each analyzed TMA spot, the field with the strongest immunostaining was selected by the observer, blinded to the clinical data and outcome of the respective patients. To limit inter-observer variability, cell counting was performed with a computerized color image analyzer (Olympus Cellsens Dimension, Olympus Medical System and Micro-Imaging Group, Hamburg, Germany). A x20 objective was used to take one microphotograph of the area of interest. A minimal object size of 50 pixels was required to count positive nuclei. Vessels and microcalcifications were excluded from the analysis. The percentage of positive and negative cells were automatically computed by the color image analyzer. A mean LI was calculated for each case. Additionally, in order to validate this computer-based LI, manual Ki-67 and MCM6 LI were evaluated in 50 randomly selected cases, by counting 1000 cells in TMA spots.

Statistical analysis

Statistical analyses were performed using IBM SPSS Statistics for Windows, Version 23.0 (IBM Corp., Armonk, NY, USA).

Because the quantitative variables did not pass the Kolmogorov–Smirnov normality test, non-parametric tests

were used. Spearman correlation test was used to explore the correlation between Ki-67 LI, MCM6 LI and the MI. The concordance between image analysis and manual LI was evaluated with the intraclass correlation coefficient. The correlation between MCM6 and Ki-67 LI and WHO grade was evaluated with the Mann–Whitney Wilcoxon test. Overall survival (OS) analyses were performed with Kaplan–Meier estimation (log-rank test) and the Cox model using univariate and multivariate analyses. For Ki-67 and MCM6 LI, the optimal threshold was computed using the Cutoff Finder online tool (8), in order to separate patients in two groups. For Cox multivariate analyses, only variables which were significant on univariate analyses and WHO grade were integrated into the model. Survival analyses were performed in the POLA cohort of IDHmut+/1p19qcode1 AO, then in the IDHmut+/1p19qcode1 OII cohort. A *P*-value (*P*) of less than 0.05 was considered statistically significant.

Transcriptomic analyses

POLA cohort: Gene expression data from POLA (29) were downloaded from <http://gliovis.bioinfo.cnio.es/> under the “Kamoun” and “POLA Network” tags. From these publicly available data, we identified 68 samples satisfying the following phenotypic criteria: histology = oligodendroglioma, grade = III (anaplastic), co-deletion 1p-19q status = yes, IDH1 or IDH2 status = mutant. These data were normalized (lowess algorithm) against a median profile of all 68 samples and further underwent descriptive statistics, which helped define groups of samples before proceeding with downstream analyses. Hence, all samples were individually labeled MCM6- and MKI67-up or -down based on their relative MCM6 and MKI67 expression (Supplementary Figure S1).

K-means clustering, functional annotations, enrichments computations, differential expression statistics and renderings were achieved using protocols and tools as described before (20). Further hierarchical clustering was applied for each significant k-means cluster to evaluate the level of correlation and quickly delineate gene or sample outliers in each gene signature.

Differential expression *P*-values were computed on normalized data using a two-way t-test between both MCM6 and MKI67 up and down groups. These were adjusted to allow for false discovery rate (FDR) using the Benjamini–Hochberg procedure and FDR < 0.01 was considered to indicate statistical significance.

Linear correlations between MCM6 and MKI67 expression levels were performed with Pearson’s method, while Spearman’s rank correlation coefficients were used to explore the dependence between both MCM6 and MKI67 gene expressions with their respective MCM6 and Ki-67 immunohistochemical LI.

TCGA cohort: Additionally, in order to evaluate the results obtained on the POLA cohort, further analyses were run on a subset of The Cancer Genome Atlas Lower Grade Glioma cohort (TCGA-LGG). From the available RNA-Seq processed data (FPKM-UQ normalized counts), 98 samples corresponded to unique cases with the following criteria:

IDH1 and/or IDH2 mutated, presence of the 1p-19q codeletion, and clearly clinically labeled as grade III and/or Anaplastic OD (35 samples) or grade II OD (63 samples). The original 60483 gene Ensembl ID were re-annotated (using <https://biotools.fr>) and their expression values were aggregated to obtain a set of unique official gene symbols. Data were then filtered to remove genes with very low expression values across samples (FPKM-UQ < 10 in more than 9/10th of the samples), which left 16345 genes. Values were re-normalized according to library size and log₂ transformed. Two datasets were then created, one set containing the 35 grade III samples, with the aim to conduct validation analyses of the POLA high-grade OD transcriptomics, and another set with the entire selected TCGA cohort of 98 grade II + grade III samples for extending the results to lower grade OD. These two data sets finally underwent the same unsupervised workflow as described above (sample ordering according to *MCM6* mRNA expression levels, k-means clustering, functional annotations, enrichment analyses).

RESULTS

Clinicopathological data

The mean age of the patients of the POLA cohort was 49 years (range 19–80) (Table 1), with a male-to-female ratio of 1.22:1. A large majority of patients had surgery first, with 33% (72/220) of them showing macroscopic total resection, 31% (68/220) subtotal resection and 21% (46/220) partial resection. As adjuvant therapy, 32% (71/220) received RT-PCV therapy and 21% (46/220) combined radiotherapy with Temozolomide (Stupp Protocol). For 29% (64/220) of them, adjuvant radiotherapy was chosen. Fourteen patients did not receive any treatment (6%; 14/220). Follow-up data were available for 220 patients and were collected over a median follow-up of 40.9 (0.3–92) months. Disease-related death occurred in 9% (19/220) of patients. Using univariate analyses, age was the only variable significantly associated with survival ($P = 0.001$; HR: 1.055 [95%CI: 1.021–1.091]) (Table 2). A high MI (at least eight mitoses per 1.6 mm²) was significantly associated with a shorter OS ($P = 0.018$; HR: 2.587 [95%CI: 1.177–5.686]). No significant correlation between OS and microvascular proliferation ($P = 0.511$; HR: 1.493 [95%CI: 0.451–4.939]) or necrosis ($P = 0.192$; HR: 1.648 [95%CI: 0.778–3.492]) was found.

In the grade II series, mean age was 44 years (range 18–81), with a male-to-female ratio of 1.21:1. Disease-related death occurred in 13% (4/30) of patients, with a median follow-up of 38.7 (2.4–79.9) months. When combining the two cohorts, WHO grade was not correlated to OS ($P = 0.642$).

MCM6 labeling index and correlation with survival

MCM6 staining was interpretable in 94% (206/220) of the cases with an average count of 1383 cells per case. Image

Table 1. Clinico-pathological characteristics and molecular data.

| Variable | Results |
|---------------------|---|
| Age (mean; min-max) | 49; 19–80 years |
| Sex | Male-to-female ratio: 1.22:1 (121/99) |
| Surgery | Biopsy: 4.1% (9/220) Total resection: 32.7% (72/220) Subtotal resection 30.9% (68/220) Partial resection 20.9% (46/220) Missing data 11.4% (25/220) |
| Type of treatment | RT-PCV: 32.3% (71/220) Radiotherapy: 29.1% (64/220) PCV: 2.3% (5/220) Stupp protocol: 20.9% (46/220) Temozolomide: 4.1% (9/220) Other: 0.5% (1/220) No treatment: 6.4% (14/220) Missing data: 3.6% (8/220) |
| Survival | Progression: 30.7% (71/220) Death: 8.2% (19/220) |
| Molecular data | <i>TERT</i> promoter mutation: 98.3% (216/220) <i>CIC</i> loss: 61% (141/220) |

RT-PCV = radiation therapy – procarbazine, CCNU (lomustine), and vincristine.

analysis-based LI was strongly correlated to manual counting (ICC: 0.864; 95%CI [0.772–0.920]). Mean MCM6 LI was 24% (range 0.1–87%; median 21.4; standard deviation 18.8) (Figure 1A,B). MCM6 LI was significantly correlated to MI ($\rho = 0.253$; $P < 0.0001$).

In the POLA cohort, log-rank survival analyses showed that patients with high MCM6 expression (upper than 50%) had significantly shorter overall survival (OS) ($P = 0.013$) (Figure 2A). Using univariate Cox model, MCM6 expression correlated inversely with OS ($P = 0.018$; HR: 3.28; 95%CI [1.22–8.83]) (Table 2). In the group of patients with grade II oligodendroglioma, a high MCM6 LI was also correlated to a shorter OS ($P = 0.001$) (Figure 3A). MCM6 LI was not significantly higher in grade III than in grade II oligodendrogliomas (23% vs. 18%; $P = 0.232$).

Ki-67 labeling index and correlation with survival

For Ki-67 LI, 91% (199/220) of the cases were interpretable. We found a high reproducibility between image analysis and manual counting (ICC: 0.900; 95%CI [0.827–0.943]). Ki-67 LI evaluated by image analysis was also strongly correlated to the Ki-67 LI previously obtained from whole slides ($\rho = 0.553$; $P < 0.0001$). The mean number of cells counted for each TMA was 1121. The mean Ki-67 LI was 6.3% (range 0.1–36.9; median 3.7; standard deviation 6.7) (Figure 1C,D). Ki-67 LI was significantly correlated to MI ($\rho = 0.275$; $P < 0.0001$) and MCM6 LI ($\rho = 0.449$; $P < 0.0001$).

The log-rank test and the univariate regression Cox model revealed that a Ki-67 LI equal to or greater than 15% was

Table 2. Univariate and multivariate Cox analyses for overall survival.

| Variable | Cox univariate (OS) | | Cox multivariate (OS) <i>Model 1</i> | | Cox multivariate (OS) <i>Model 2</i> | |
|---|---------------------|-----------------|--------------------------------------|-----------------|--------------------------------------|-----------------|
| | HR [95%CI] | <i>P</i> -value | HR [95%CI] | <i>P</i> -value | HR [95%CI] | <i>P</i> -value |
| Age | 1.055 [1.021–1.091] | 0.001* | 1.060 [1.020–1.103] | 0.003* | 1.051 [1.011–1.092] | 0.012* |
| Mitotic index $\geq 8/1.6 \text{ mm}^2$ | 2.587 [1.177–5.686] | 0.018* | 1.439 [0.538–3.851] | 0.469 | 1.588 [0.606–4.162] | 0.347 |
| MCM6 LI $\geq 50\%$ | 3.283 [1.221–8.826] | 0.018* | 2.896 [0.964–8.702] | 0.058 | | |
| Ki-67 LI $\geq 15\%$ | 3.948 [1.442–10.41] | 0.008* | 2.713 [0.935–7.875] | 0.066 | | |
| MCM6 LI $\geq 50\%$ and/or Ki-67 LI $\geq 15\%$ | 3.875 [1.603–9.370] | 0.003* | | | 2.872 [1.125–7.328] | 0.027* |

HR = hazard ratio; LI = labeling index; OS = overall survival.

*Statistically significant ($P < 0.05$).

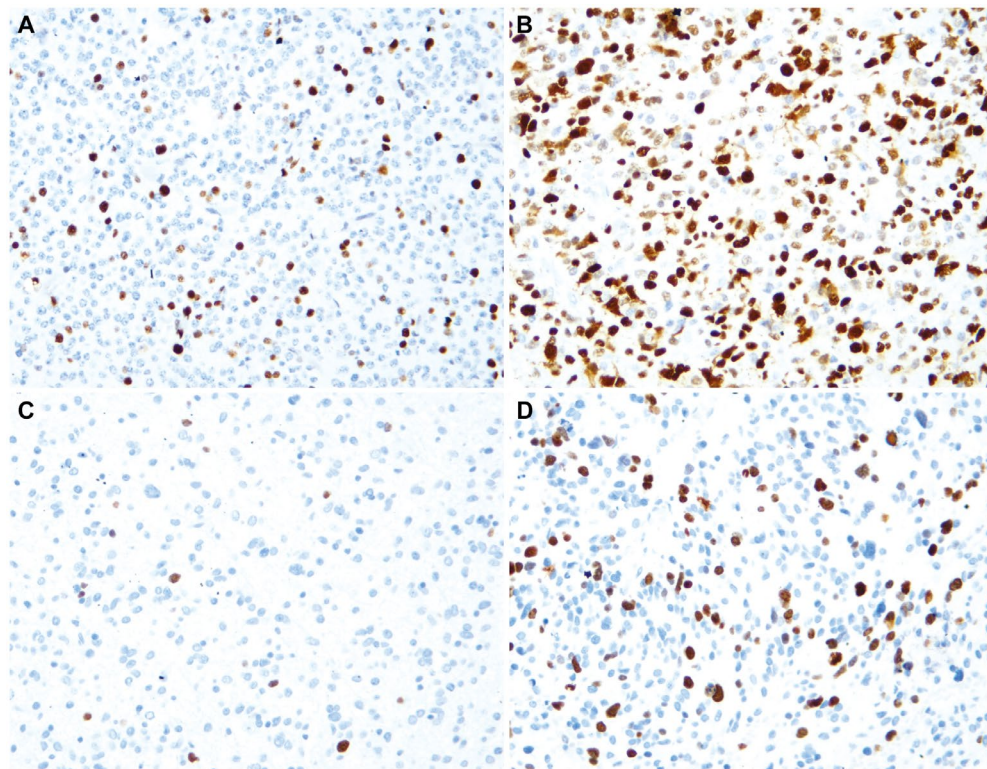


Figure 1. Immunolabeling for MCM6 and Ki-67 (immunohistochemistry, $\times 200$). A. Low MCM6 labeling index (LI). B. High MCM6 LI. C. Low Ki-67 LI. D. High Ki-67 LI (same case as B).

correlated with a shorter OS (log-rank: $P = 0.004$; Cox: $P = 0.008$; HR = 3.948; 95%CI [1.442–10.41]) (Figure 2B; Table 2). Similarly, in the group of patients with grade II oligodendroglioma, a high Ki-67 LI was correlated to shorter OS ($P = 0.027$; log-rank test) (Figure 3B). Ki-67 LI was significantly higher in grade III than in grade II tumors (6% vs. 3%; $P = 0.001$).

Multivariate survival analyses

The variables that were significant in univariate analyses (age, MI $\geq 8/1.6 \text{ m}^2$, MCM6 LI $\geq 50\%$, Ki-67 LI $\geq 15\%$) were included in the first multivariate Cox model. Only age remained significantly correlated to OS ($P = 0.003$), whereas

MCM6 and Ki-67 LI were close to significance ($P = 0.058$ and $P = 0.066$, respectively) (Table 2).

In order to evaluate if MCM6 could be an interesting marker to use in complement to Ki-67, we designed a second Cox multivariate model, with the variable “MCM6 LI $\geq 50\%$ and/or Ki-67 LI $\geq 15\%$ ”, that was strongly significant in univariate analysis (log-rank: $P = 0.001$; Cox: $P = 0.003$; HR: 3.875; 95%CI [1.603–9.370]). With this model, age and “MCM6 LI $\geq 50\%$ and/or Ki-67 LI $\geq 15\%$ ” were significantly correlated to OS ($P = 0.012$ and $P = 0.027$, respectively), but not MI ($P = 0.347$) (Figure 2C; Table 2).

Additionally, we evaluated the prognostic value of MCM6 and Ki-67 LI in all cases of IDHmut+/1p19qcodeleted oligodendrogliomas, including grade II and III tumors. In a

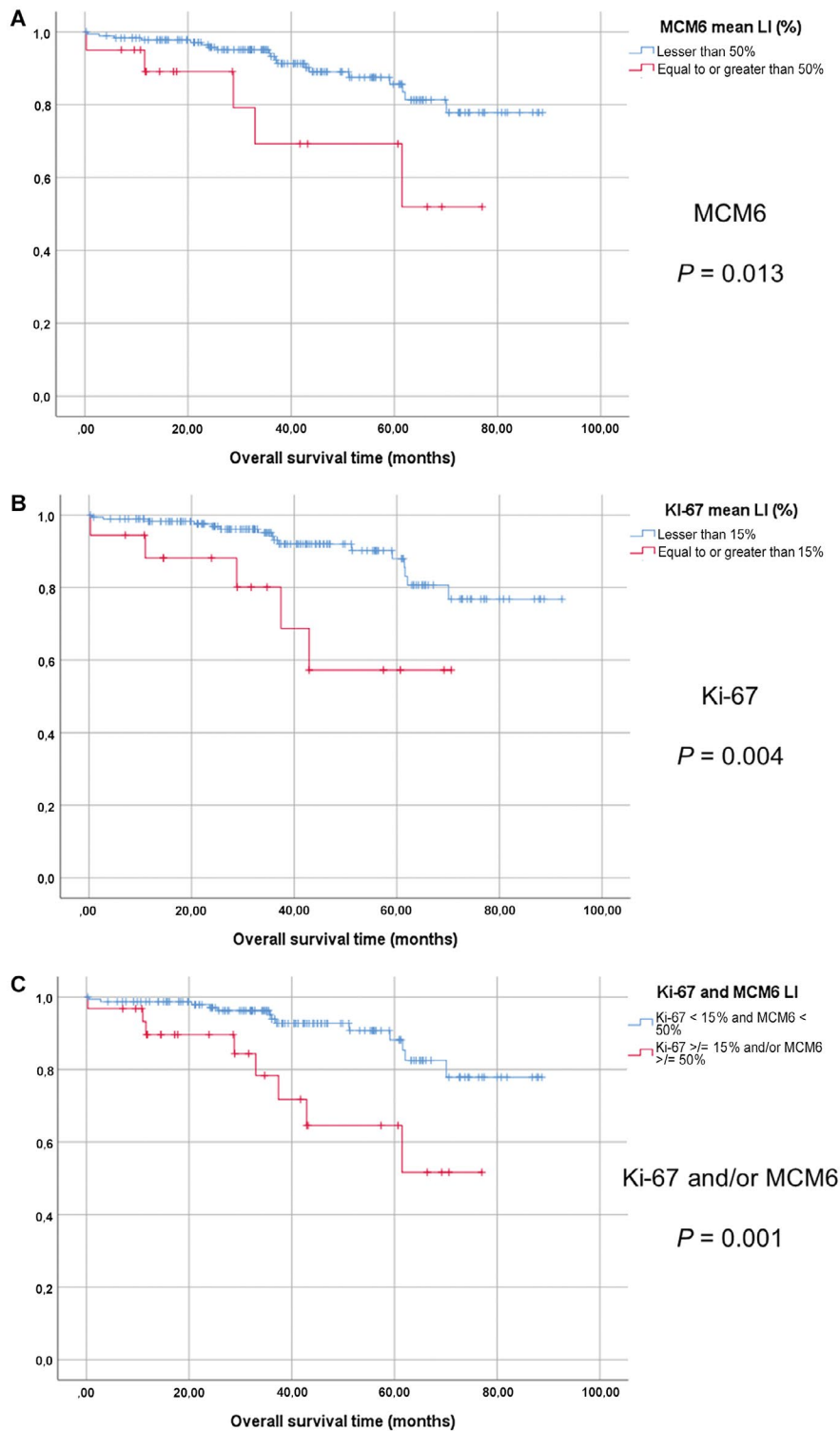


Figure 2. Survival analyses in the POLA cohort of anaplastic oligodendrogliomas. Kaplan-Meier curves with log-rank tests (overall survival). A. MCM6 labeling index, 50% threshold (LI). B. Ki-67 LI, 15% threshold. C. MCM6 LI \geq 50% and/or Ki-67 LI \geq 15% vs. MCM6 $<$ 50% and Ki-67 LI $<$ 15%.

multivariate model including age, MI, WHO grade and the two proliferation markers, we found that age ($P = 0.022$) and MCM6 LI \geq 50% and/or Ki-67 LI \geq 15% ($P = 0.001$;

HR: 4.148; 95%CI [1.735–9.920] were significantly associated with OS, but not WHO grade ($P = 0.108$) or MI ($P = 0.637$).

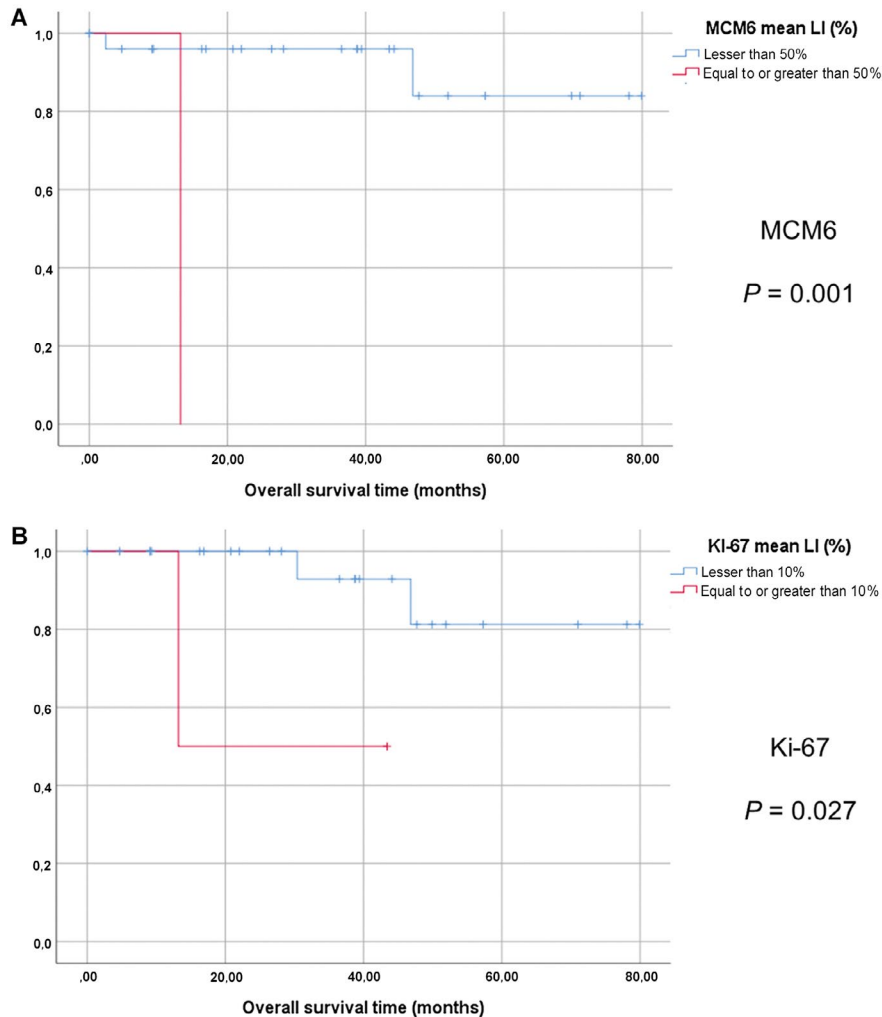


Figure 3. Survival analyses the cohort of grade II oligodendrogliomas. Kaplan-Meier curves with log-rank tests (overall survival). A. MCM6 labeling index, 50% threshold (LI). B. Ki-67 LI, 10% threshold.

Transcriptomics in the POLA cohort

For both *MCM6* and *MKI67*, we expected positive correlations between their LI and mRNA level in AO cases for which both transcriptomic data and LI were available. The Spearman tests indeed confirmed such correlations ($\rho = 0.43$, $P = 0.003$, $n = 46$; and $\rho = 0.63$, $P = 4.7 \times 10^{-5}$, $n = 38$, respectively) (Supplementary Figure S2). A highly positive correlation was also found between the mRNA level of *MCM6* and that of the *MKI67* in the AO transcriptomes of the POLA network ($n = 68$; Pearson’s test: 0.69; $P = 5.6 \times 10^{-11}$) (Supplementary Figure S3).

Molecular events associated with differential expressions of either *MCM6* or *MKI67* in these AO samples were subsequently analyzed ($n = 68$). This was achieved using the median expression levels for *MCM6* and *MKI67* as “up” and “down” subgroup delimiters (Supplementary Figure S1) in two separate analyses based on the relative expressions of *MCM6* and *MKI67*. When the median *MCM6* mRNA level was used to organize the 68 AO samples, 34 were classified

and labeled as *MCM6*-down (sample expression < median expression), and the remaining 34 as *MCM6*-up (expression > median). The same was applied for *MKI67*. In these two analyses, k-means clustering coupled with a distance computation based on the weighted correlation method, permitted the identification of clusters with distinct molecular functions differentiating the “up” from the “down” *MCM6* or *MKI67*-expresser AO (Figure 4). Remarkably, these *MCM6*- and *MKI67* gradient-driven clusterings resulted in individual clusters sharing high level of identity, as the clusters produced between the *MCM6* and *MKI67* series of experiments overlapped with each other (ranging from 85% to 99%, the most significant clusters presenting with the greatest identity) (Figure 4). Moreover, among the 10 clusters identified in each series (from c0 to c9), 2 clusters of upregulated genes (c3 and c7) and 3 clusters of downregulated genes (c1, c2 and c6) were highly conserved between the two series (98%, 99%, 97%, 97%, 96%, respectively; Figure 4). Further functional annotation of the up- and downregulated clusters revealed that tumors expressing higher levels of *MCM6* and *MKI67* were

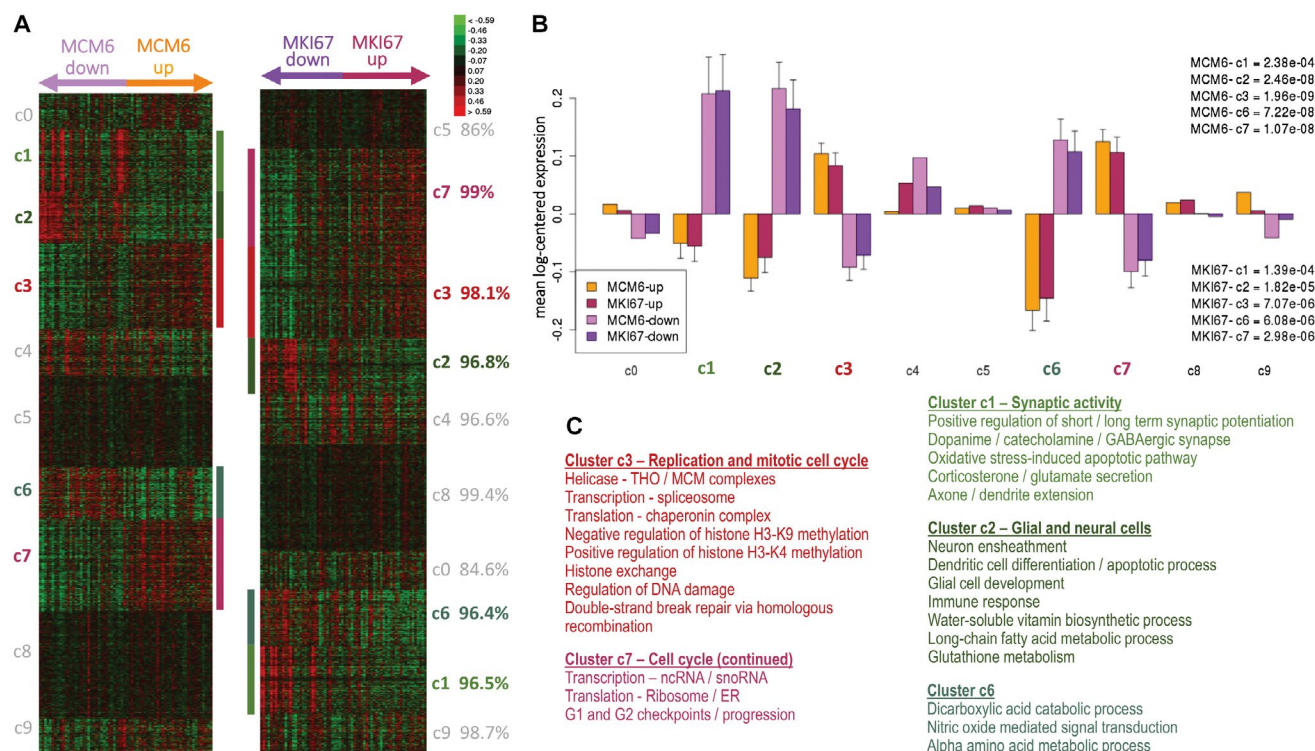


Figure 4. K-means clustering from MCM6 and MKI67 expression gradients (from lowest to highest) of 68 transcriptomes of anaplastic oligodendrogliomas from the POLA network. The two independent K-means clustering each delineated five significant groups of co-expressed genes ($P < 0.01$) showing highly correlated expression profiles. **A.** Heatmap of the ten identified k-means clusters in the two clustering results, and lowest identity (in %) found for each cluster (green, red and black indicate downregulated, upregulated, and median genes, respectively). **B.** Mean gene expression (overall with standard

error at the mean) for each cluster in MCM6 and MKI67 analyses where both upregulated samples for MCM6 or MKI67 are compared to their downregulated counterparts (AU – arbitrary units). Upregulated and downregulated samples are defined relatively to the median gene expression for either MCM6 or MKI67. **C.** Overview of the most relevant functional annotations for the significantly over- and under-expressed clusters (in red and green hues, respectively, all $p(FDR) \leq 0.01$).

also enriched with genes controlling replication and cell cycle (c3 and c7), but downregulated with genes associated with synaptic activity (c1), neuron ensheathment, glial cell development, immune and inflammatory response, vitamin biosynthetic process (c2), and alpha amino acid metabolic process (c6) ($FDR < 0.0001$) (Supplementary Table S1).

Additionally, we explored differential expression statistics (two-sided t-test) between MCM6-up and MCM6-down, and between MKI67-up and MKI67-down samples. Four significant gene lists were produced (all $FDR < 0.01$), one list for over- and one for under-expressed genes in MCM6-up samples (871 and 461 genes; fold changes $> 4/3$ and $< 3/4$, respectively), and likewise for MKI67-up samples (352 and 237 genes, respectively) (Supplementary Table S2). MCM6 overexpressed samples presented with a significant enrichment in genes involved in cell cycle functions (Table 3), including most notably DNA replication, mitotic centrosome separation and mitotic chromosome condensation and genes involved in internal ribosome entry site (IRES) dependent translational initiation. Tumors harboring lower MCM6 expression showed significant upregulation of pathways involved in glial differentiation and immune response, such

as microglial cell activation, myelination, oligodendrocyte development and oligodendrocyte differentiation. Similarly, tumors with higher expression of MKI67 (Table 4) were enriched in genes involved with cell cycle functions such as DNA strand elongation in DNA replication during cell cycle, pre-replicative complex assembly, mitotic chromosome condensation and MCM complex. Tumors with lower MKI67 expression were significantly enriched in genes involved in beta-amyloid binding, synaptic vesicle, axon terminus, trans-synaptic signaling, neuronal cell body and cell projection.

When focusing on genes associated with a pro-neural signature, such as SOX2, SOX4, SOX11, OLIG1, OLIG2, INSM1, FERMT1, DCX, CTTNBP2, ATOH8 and ASCL1, we found a significant overexpression of these genes in tumors showing higher levels of MCM6 and MKI67 ($FDR < 0.01$) (Supplementary Figure S4A). Surprisingly, a number of genes involved in immunological responses were significantly downregulated in these tumors (CX3CRI, TLR4, SYK, FAS, HSPA2, CEBPB, TRIM59, ITGB5, PLP1, C3ARI, PREX1, MND, GAB2, VAMP3; $FDR < 0.01$) (Supplementary Figure S4B). Genes controlling the production of molecular mediators involved in inflammatory response were more significantly

Table 3. Top 12 Gene Ontology functional annotations associated with the expression of MCM6 (sorted by fold enrichment).

| GO biological process | Fold enrichment | FDR |
|---|-----------------|---------|
| <i>Enrichment in tumors showing MCM6 higher expression</i> | | |
| Cell cycle DNA replication initiation (GO:1902292) | 22.1 | <0.0001 |
| DNA strand elongation involved in cell cycle DNA replication (GO:1902296) | 21.7 | 0.0001 |
| Ndc80 complex (GO:31262) | 21.7 | 0.0001 |
| Pre-replicative complex assembly (GO:36388) | 21.3 | <0.0001 |
| Condensed nuclear chromosome kinetochore (GO:778) | 15.2 | <0.0001 |
| Mitotic centrosome separation (GO:7100) | 15.2 | 0.001 |
| Mitotic chromosome condensation (GO:7076) | 14.8 | <0.0001 |
| IRES-dependent translational initiation (GO:2192) | 14.6 | 0.0001 |
| Aster (GO:5818) | 13.8 | 0.0001 |
| Exodeoxyribonuclease activity (GO:4529) | 12.6 | 0.003 |
| Mitotic prophase (GO:88) | 12.1 | <0.0001 |
| Regulation of transcription involved in G1/S transition (GO:83) | 11.9 | <0.0001 |
| <i>Enrichment in tumors showing MCM6 lower expression</i> | | |
| Myelin sheath adaxonal region (GO:35749) | 11.2 | 0.009 |
| Negative regulation of inclusion body assembly (GO:90084) | 8.7 | 0.02 |
| Sodium ion export from cell (GO:36376) | 8.7 | 0.02 |
| Positive regulation of organic acid transport (GO:32892) | 8.2 | 0.02 |
| Microglial cell activation (GO:1774) | 8.4 | <0.0001 |
| Macrophage activation involved in immune response (GO:2281) | 8.2 | 0.009 |
| Central nervous system myelination (GO:22010) | 7.6 | 0.002 |
| Positive regulation of myelination (GO:31643) | 6.5 | 0.02 |
| Main axon (GO:44304) | 4.6 | <0.0001 |
| Proteoglycan binding (GO:43394) | 4.5 | 0.01 |
| Oligodendrocyte development (GO:14003) | 4.2 | 0.005 |
| Positive regulation of glial cell differentiation (GO:45687) | 4.0 | 0.02 |

FDR = false discovery rate; GO = gene ontology.

downregulated with *MCM6*-up than *MKI67*-up (*EPHX2*, *APOD*, *VAMP3*, *SYK*, *ALOX5*, *DUSP10*, *SNX6*, *ADORA3*, *ALOX5AP*, *TNF*, *LYN*, *BTK*, *FCER1G*, *IL17RA* and the pro-inflammatory mediator *IL17D*; FDR < 0.01) (Supplementary Table S2).

Other gene signatures were also found to overexpress with *MCM6* and *MKI67* high transcription, such as epigenetic markers (*DNMT1A*, *EZH2*, *TYMS*, *DHFR*; FDR < 0.01) and cell cycle progression key protagonists (all *MCMs*, *PCNA*, *CCNBI*, *CCND1*, *CDK1*, *CDK4*; FDR < 0.01), whereas myelination and glial cell differentiation genes were under-expressed with *MCM6* (FDR < 0.01) but less clearly with *MKI67* high levels, which is in accordance with the functional annotations reported above (Supplementary Figures S4B,C,E,F). Strongly upregulated KEGG pathways were all associated with an *MCM6* or *MKI67* overexpression (ribosome, RNA transport, splicing and degradation, DNA replication and repair, P53 signaling; *q*-value < 0.05). Both *MCM6*-up and *MKI67*-up sets of significantly disturbed pathways were nearly identical, with cell cycle controlling genes showing the same overexpression patterns (Supplementary Figure S5).

Confirmation analyses based on TCGA data

To validate the observations made on the POLA cohort, we ran a validation analysis with 98 similar cases identified in TCGA (The Cancer Genome Atlas) database. These were all identified as IDH1/IDH2 codeleted OD cases and included

35 fully annotated grade III and 63 grade II samples. Our survival analyses of the 98 TCGA cases showed that similar to that observed in our own grade II/III cohort, high levels of *MCM6* mRNA (equal to or greater than the median expression; arbitrary unit) indeed correlated to a shorter OS ($P = 0.027$) (Supplementary Figure S6A). However, the mRNA level of *MKI67* in the TCGA samples did not correlate with OS ($P = 0.398$) (Supplementary Figure S6B). WHO grade did not correlate to survival ($P = 0.617$) (Supplementary Figure S6C). Only age was independently correlated to survival (Cox multivariate analysis, $P = 0.007$). *MCM6* and *MKI67* mRNA levels were strongly correlated ($\rho = 0.623$; $P < 0.0001$). No significant correlation existed between the WHO grade and the mRNA level of either *MCM6* or *MKI67* ($P > 0.50$).

We also compared the transcriptomic signatures obtained with anaplastic POLA samples with the 35 grade III independent cases retrieved from TCGA (Supplementary Figure S7). We did so by conducting the analyses with the same unsupervised protocols on the TCGA data set as were applied to the POLA study. As sample grouping according to *MCM6* and *MKI67* median expression levels led to the same configuration, results for both comparisons were fused as one. Similar molecular signatures were indeed uncovered in TCGA samples, each signature presenting with an enrichment with its POLA counterpart ranging from 3.3 to 7.6 times higher than expected (all $P < 1 \times 10^{-100}$, Fisher's exact test). These showed a downregulation of inflammation, glial differentiation,

Table 4. Top 12 Gene Ontology functional annotations associated with the expression of MKI67 (sorted by fold enrichment).

| GO biological process | Fold enrichment | FDR |
|---|-----------------|---------|
| <i>Enrichment in tumors showing MKI67 higher expression</i> | | |
| Condensin complex (GO:796) | 50.2 | <0.0001 |
| Replication fork protection complex (GO:31298) | 42.1 | <0.0001 |
| DNA strand elongation involved in cell cycle DNA replication (GO:1902296) | 40.1 | <0.0001 |
| Ndc80 complex (GO:31262) | 40.1 | <0.0001 |
| Pre-replicative complex assembly (GO:36388) | 35.1 | <0.0001 |
| Leading strand elongation (GO:6272) | 35.1 | <0.0001 |
| Condensed nuclear chromosome kinetochore (GO:778) | 31.6 | <0.0001 |
| MCM complex (GO:42555) | 28.1 | 0.0001 |
| Mitotic centrosome separation (GO:7100) | 28.1 | 0.0001 |
| Mitotic chromosome condensation (GO:7076) | 27.5 | <0.0001 |
| Kinetochore microtubule (GO:5828) | 25.5 | 0.0001 |
| Aster (GO:5818) | 25.5 | 0.0001 |
| <i>Enrichment in tumors showing MKI67 lower expression</i> | | |
| Regulation of inclusion body assembly (GO:90083) | 12.3 | 0.03 |
| Beta-amyloid binding (GO:1540) | 10.5 | 0.005 |
| Neurotrophin TRK receptor signaling pathway (GO:48011) | 7.9 | 0.04 |
| Import into cell (GO:98657) | 6.6 | 0.01 |
| Sodium ion transmembrane transport (GO:35725) | 4.7 | 0.03 |
| Synaptic vesicle (GO:8021) | 4.1 | 0.007 |
| Postsynaptic specialization (GO:99572) | 3.7 | 0.001 |
| Axon part (GO:33267) | 3.7 | <0.0001 |
| Excitatory synapse (GO:60076) | 3.7 | 0.001 |
| Myelin sheath (GO:43209) | 3.4 | 0.01 |
| Dendrite (GO:30425) | 2.6 | 0.001 |
| Trans-synaptic signaling (GO:99537) | 2.5 | 0.001 |

FDR = false discovery rate; GO = gene ontology.

myelin sheath and synaptic activity in tumors that overexpressed *MCM6* and/or *MKI67*, and an upregulation of mitotic cell cycle and DNA replication (all FDR < 0.01).

We further asked if these results extended to grade II cases and applied the same experimental protocol on TCGA combined grades II/III cohort (n = 98; Supplementary Figure S8). Clusters of genes involved in mitotic cell cycle/replication, myelin sheath/glia cell differentiation and axoneme/oxacid metabolic process were indeed strongly differential between *MCM6*-down and *MCM6*-up groups (all FDR < 0.01), and presented with high identities with their POLA counterparts (73.6%, 60.6% and 48.2%, respectively). However, we did not find well-defined signatures such as those reported for grade III alone of both POLA and TCGA cohorts for the other clusters. The immune response/inflammation signature, in particular, was lost when including grade II samples to the mixture.

DISCUSSION

The aim of our study was to evaluate the prognostic value of *MCM6* and *Ki-67* LI in AOs. Previously, other members of *MCM* family, such as *MCM2*, *MCM3* and *MCM7*, have indeed been studied in gliomas, and their overexpression was associated with a poor overall prognosis; however, their applicability in clinical practice seems to be unclear (14, 16, 27). The prognostic value of *MCM6* has been confirmed in various

types of brain tumors like meningiomas, adamantinomatous craniopharyngiomas and gliomas (9, 21, 48). In the present study, we specifically focused on AOs with the presence of defined mutations of *IDH1/2* mutations and 1p/19q codeletion to avoid confusing factors due to molecular alterations. Indeed, *IDH1/2* mutations and 1p/19q codeletion are known to correlate with better outcome, due notably to a better response to adjuvant chemotherapy. Only few prognostic markers have been reported in the specific group of *IDHmut+/1p19qcodelet* AO. In this work, PFS was not assessed, because a consensual definition of progression in glioma is still lacking (1, 7, 28).

In this study, we found a good correlation between the mean LIs of *MCM6* and *Ki-67*. *MCM6* LI was always higher than *Ki-67* LI in a given tumor (Figure 1). This is consistent with data of the literature, and is due to the fact that *MCMs* are expressed earlier in the cell cycle (15, 30). Furthermore, we have identified a cutoff point at 50% *MCM6* LI as the optimal criteria for survival prediction: at greater than a LI of 50%, *MCM6* overexpression correlated with a shorter overall survival. Based on the results we obtained earlier in meningioma, in which high *MCM6* LI were found correlated with survival (21), this marker may even be applicable to other brain tumor types. Consequently, this high labeling index of *MCM6* at 50% threshold can be considered as an easy-to-use tool for routine practice of the pathology laboratories, in complement to *Ki-67*.

We also found that high mean LIs of *Ki-67* were associated with poor outcome, with a threshold of 15%. This

result is consistent with previous studies using the EORTC (European Organization for Research and Treatment of Cancer) Brain Tumor Group (40).

Given the results reported above, it shall be noted that although Ki-67 LI had good inter-observer agreement in previous studies (11, 39), there is no consensual method for counting Ki-67 LI in AO. Usually, most of the neuropathologists select areas showing the highest proliferation. Here, in order to have a more reproducible counting method for both Ki-67 and MCM6, we adapted computerized color image analyses based on previous results for Ki-67 cell scoring (6, 36). Consequently, a wide area was analyzed for each TMA spot. However, as we were not sure whether the selected spots corresponded to areas with the highest cell proliferation (despite the fact that individual spots were made with histologically representative samples of the tumors), we determined in our series the correlation between the Ki-67 LI obtained from TMA and the one obtained from whole slides; we found that these values correlated significantly ($\rho = 0.553$; $P < 0.0001$; data not shown), confirming the adequacy of our prepared TMA spots.

Multivariate analyses showed that MCM6 may be an interesting marker to use in association to Ki-67. Indeed, tumors harboring MCM6 LI $\geq 50\%$ and/or Ki-67 LI $\geq 15\%$ were significantly correlated to shorter survival, both in univariate and multivariate analyses. High MCM6 and Ki-67 LI were also correlated to shorter survival in grade II tumors, while in our study WHO grade was not significantly correlated to survival. However, these results are limited by a relatively short median follow-up time and a low number of OS events, thus the observed survival differences were based on few patients. Another limitation is that we used a statistical method that specifically seeks for the best cutoff in a given data set, which may not be applicable in another cohort. Further studies are needed in order to confirm the validity of these thresholds.

Analyses of the transcriptome data of the POLA grade III cohort showed that *MCM6* and/or *MKI67* overexpressing tumors share near identical whole transcriptional profiles, in spite of a correlation between *MCM6* and *MKI67* mRNA levels not being perfect. These tumors upregulated genes linked to DNA replication during the cell cycle (including all *MCMs*), DNA strand elongation, pre-replicative complex assembly, mitotic centrosome condensation and separation or regulation of helicase activity. This is consistent with the highly proliferative activity of these aggressive cancers. In addition, the *MCM6*-up and *MKI67*-up tumors of the POLA AO cohort overexpressed pro-neuronal differentiation genes such as *SOX4*, *SOX11*, *INSM1* and *ASCL1*. These findings are consistent with the pro-neuronal signature of the AO previously highlighted by Bielle *et al*. These authors identified a subgroup of AO overexpressing neuronal intermediate progenitor genes, associated with immunohistochemical similarities to embryonic subventricular zone, expression of *INSM1* and no expression of *SOX9* (5).

On the contrary, in AO cases showing an overall lower expression of *MCM6* and/or *MKI67*, transcriptomic analyses revealed enrichments of genes involved in myelin sheath production, myelination or oligodendroglial differentiation. These results suggest that both *MCM6*-down and

MKI67-down tumors lack a pro-neuronal signature, and unlike their *MCM6*-*MKI67*-up counterparts, are well-differentiated oligodendroglial-like tumors.

In the *MCM6*-down subgroup, we also found genes like *CX3CR1*, *TLR4* and *SYK*, involved in immune response and microglial cells activation. Such downregulations in immune responsive genes have been observed in other types of glioma. For example, in murine models, loss of *CX3CR1* expression promoted gliomagenesis in glioblastoma with pro-neuronal signature through larger inflammatory monocytes accumulation (17). Lower levels of *TLR4*, a member of the toll-like receptors involved in macrophagic immune response, have been implicated in the immune evasion of glioblastoma stem cells (3). The immune evasion in high-grade gliomas is well documented. The non-neoplastic cells of the glioma microenvironment, such as fibroblasts, endothelial cells or microglial cells, produce survival and growth factors, helping tumors cells to grow and infiltrate the brain parenchyma (23). The stimulatory role of spleen tyrosine kinase receptors (*SYK*) in gliomagenesis, brain invasion, and recruitment of immune cells has recently been studied in glioblastoma stem cells by Moncayo *et al* using *SYK*-inhibitors, but their involvement has never been specifically studied in AO (37). In another study, *SYK* appeared as a tumor suppressor gene in breast carcinomas (13). First-generation *SYK*-inhibitors have been successfully tested in some hematologic malignancies, as B-acute lymphoid leukemia and chronic lymphocytic lymphoma (25, 44). The assessment of their efficiency in high-grade gliomas needs further investigations.

Finally, the predictive prognostic power of *MCM6* and/or *MKI67* was tested using a TCGA cohort of *IDH1*-*IDH2*-codel glioma composing of both grade II ($n = 68$) and III ($n = 35$) tumors. We found that high *MCM6* expression indeed correlated with OS, but not *MKI67*.

CONCLUSION

In this study, we assessed the prognostic value of MCM6 and Ki-67 LI in *IDH*-mutant and 1p/19q codeleted AOs of the POLA cohort. Our multivariate analyses showed that the overexpression of MCM6 and/or Ki-67 was independently correlated to shorter survival. The prognostic value of MCM6 was confirmed in TCGA grade II–III *IDH*-mutant and 1p/19q codeleted gliomas. These two easy-to-use and cost-effective markers could thus be used concurrently in routine pathology practice. Potentially, these markers could also be integrated into therapeutic as well as clinicoradiological monitoring strategies to improve disease outcomes. We also would like to underline the important new insight gained from the transcriptomic analyses of the AO, which is that AO with high proliferation have downregulated immune response and lower microglial cells activation.

ACKNOWLEDGMENTS

The authors wish to thank all the team of the CHRU Nancy Pathology Department for technical support, the members of

the POLA network for contributing case material and Marion Divoux for her help in manuscript preparation. The results shown here are in part based upon data generated by the TCGA Research Network: <http://cancergenome.nih.gov/>.

CONFLICT OF INTEREST

The authors have no conflict of interest to declare.

REFERENCES

- Abdulla S, Saada J, Johnson G, Jefferies S, Ajithkumar T (2015) Tumour progression or pseudoprogression? A review of post-treatment radiological appearances of glioblastoma. *Clin Radiol* **70**:1299–1312.
- Alentorn A, Dehais C, Ducray F, Carpentier C, Mokhtari K, Figarella-Branger D *et al* (2015) Allelic loss of 9p21.3 is a prognostic factor in 1p/19q codeleted anaplastic gliomas. *Neurology* **85**:1325–1331.
- Alvarado AG, Thiagarajan PS, Mulkearns-Hubert EE, Silver DJ, Hale JS, Alban TJ *et al* (2017) Glioblastoma cancer stem cells evade innate immune suppression of self-renewal through reduced TLR4 expression. *Cell Stem Cell* **20**:450–461.
- Bettegowda C, Agrawal N, Jiao Y, Sausen M, Wood LD, Hruban RH *et al* (2011) Mutations in CIC and FUBP1 contribute to human oligodendroglioma. *Science* **333**:1453–1455.
- Bielle F, Ducray F, Mokhtari K, Dehais C, Adle-Biassette H, Carpentier C *et al* (2017) Tumor cells with neuronal intermediate progenitor features define a subgroup of 1p/19q co-deleted anaplastic gliomas. *Brain Pathol* **27**:567–579.
- Blaker YN, Brodtkorb M, Maddison J, Hveem TS, Nesheim JA, Mohn HM *et al* (2015) Computerized image analysis of the Ki-67 proliferation index in mantle cell lymphoma. *Histopathology* **67**:62–69.
- Brandsma D, Stalpers L, Taal W, Sminia P, Van den Bent MJ (2008) Clinical features, mechanisms, and management of pseudoprogression in malignant gliomas. *Lancet Oncol* **9**:453–461.
- Budczies J, Klauschen F, Sinn BV, Györfy B, Schmitt WD, Darb-Esfahani S, Denkert C (2012) Cutoff finder: A comprehensive and straightforward web application enabling rapid biomarker cutoff optimization. *PLoS ONE* **7**:e51862.
- Cai HQ, Chen ZJ, Zhang HP, Wang PF, Zhang Y, Hao JJ *et al* (2018) Overexpression of MCM6 predicts poor survival in patients with glioma. *Hum Pathol* **78**:182–187.
- Cancer Genome Atlas Research Network, Brat DJ, Verhaak RGW, Aldape KD, Yung WKA, Salama SR *et al* (2015). Comprehensive, integrative genomic analysis of diffuse lower-grade gliomas. *N Engl J Med* **372**:2481–2498.
- Coleman KE, Brat DJ, Cotsonis GA, Lawson D, Cohen C (2006) Proliferation (MIB-1 expression) in oligodendrogliomas: assessment of quantitative methods and prognostic significance. *Appl Immunohistochem Mol Morphol* **14**:109–114.
- Coons SW, Johnson PC, Pearl DK (1997) The prognostic significance of Ki-67 labeling indices for oligodendrogliomas. *Neurosurgery* **41**:878–884; discussion 884–885.
- Coopman PJ, Do MT, Barth M, Bowden ET, Hayes AJ, Basyuk E *et al* (2000) The Syk tyrosine kinase suppresses malignant growth of human breast cancer cells. *Nature* **406**:742–747.
- Erkan EP, Ströbel T, Lewandrowski G, Tannous B, Madlener S, Czech T *et al* (2014) Depletion of minichromosome maintenance protein 7 inhibits glioblastoma multiforme tumor growth in vivo. *Oncogene* **33**:4778–4785.
- Eward KL, Obermann EC, Shreeram S, Loddo M, Fanshawe T, Williams C *et al* (2004) DNA replication licensing in somatic and germ cells. *J Cell Sci* **117**:5875–5886.
- Facoetti A, Ranza E, Benericetti E, Ceroni M, Tedeschi F, Nano R (2006) Minichromosome maintenance protein 7: a reliable tool for glioblastoma proliferation index. *Anticancer Res* **26**:1071–1075.
- Feng X, Szulzewsky F, Yerevanian A, Chen Z, Heinzmann D, Rasmussen RD *et al* (2015) Loss of CX3CR1 increases accumulation of inflammatory monocytes and promotes gliomagenesis. *Oncotarget* **6**:15077–15094.
- Figarella-Branger D, Mokhtari K, Dehais C, Carpentier C, Colin C, Jouveta A *et al* (2016) Mitotic index, microvascular proliferation, and necrosis define 3 pathological subgroups of prognostic relevance among 1p/19q co-deleted anaplastic oligodendrogliomas. *Neuro Oncol* **18**:888–890.
- Figarella-Branger D, Mokhtari K, Dehais C, Jouveta A, Uro-Coste E, Colin C *et al* (2014) Mitotic index, microvascular proliferation, and necrosis define 3 groups of 1p/19q codeleted anaplastic oligodendrogliomas associated with different genomic alterations. *Neuro Oncol* **16**:1244–1254.
- Gauchotte G, Hergalant S, Vigouroux C, Casse JM, Houlgatte R, Kaoma T *et al* (2017) Cytoplasmic overexpression of RNA-binding protein HuR is a marker of poor prognosis in meningioma, and HuR knockdown decreases meningioma cell growth and resistance to hypoxia. *J Pathol* **242**:421–434.
- Gauchotte G, Vigouroux C, Rech F, Battaglia-Hsu SF, Soudant M, Pinelli C *et al* (2012) Expression of minichromosome maintenance MCM6 protein in meningiomas is strongly correlated with histologic grade and clinical outcome. *Am J Surg Pathol* **36**:283–291.
- Gleize V, Alentorn A, Connen de Kérillis L, Labussière M, Nadaradjane AA, Mundwiller E *et al* (2015) CIC inactivating mutations identify aggressive subset of 1p19q codeleted gliomas. *Ann Neurol* **78**:355–374.
- Hambardzumyan D, Gutmann DH, Kettenmann H (2016) The role of microglia and macrophages in glioma maintenance and progression. *Nat Neurosci* **19**:20–27.
- Helfenstein A, Frahm SO, Krams M, Drescher W, Parwaresch R, Hassenpflug J (2004) Minichromosome maintenance protein (MCM6) in low-grade chondrosarcoma: distinction from enchondroma and identification of progressive tumors. *Am J Clin Pathol* **122**:912–918.
- Hoellenriegel J, Coffey GP, Sinha U, Pandey A, Sivina M, Ferrajoli A *et al* (2012) Selective, novel Spleen tyrosine kinase (Syk) inhibitors suppress chronic lymphocytic leukemia B cell activation and migration. *Leukemia* **26**:1576–1583.
- Hotton J, Agopiantz M, Leroux A, Charra-Brunaud C, Marie B, Busby-Venner H *et al* (2018) Minichromosome maintenance complex component 6 (MCM6) expression correlates with histological grade and survival in

- endometrioid endometrial adenocarcinoma. *Virchows Arch* **472**:623–633.
27. Hua C, Zhao G, Li Y, Bie L (2014) Minichromosome Maintenance (MCM) Family as potential diagnostic and prognostic tumor markers for human gliomas. *BMC Cancer* **14**:526.
 28. Jain R, Narang J, Sundgren PM, Hearshen D, Saksena S, Rock JP *et al* (2010) Treatment induced necrosis versus recurrent/progressing brain tumor: going beyond the boundaries of conventional morphologic imaging. *J Neurooncol* **100**:17–29.
 29. Kamoun A, Idbah A, Dehais C, Elarouci N, Carpentier C, Letouzé E *et al* (2016) Integrated multi-omics analysis of oligodendroglial tumours identifies three subgroups of 1p/19q co-deleted gliomas. *Nat Commun* **7**.
 30. Kingsbury SR, Loddo M, Fanshawe T, Obermann EC, Prevost AT, Stoerber K, Williams GH (2005) Repression of DNA replication licensing in quiescence is independent of geminin and may define the cell cycle state of progenitor cells. *Exp Cell Res* **309**:56–67.
 31. Labib K, Kearsley SE, Diffley JF (2001) MCM2-7 proteins are essential components of prereplicative complexes that accumulate cooperatively in the nucleus during G1-phase and are required to establish, but not maintain, the S-phase checkpoint. *Mol Biol Cell* **12**:3658–3667.
 32. Labreche K, Simeonova I, Kamoun A, Gleize V, Chubb D, Letouzé E *et al* (2015) TCF12 is mutated in anaplastic oligodendroglioma. *Nat Commun* **6**.
 33. Lindner K, Gregán J, Montgomery S, Kearsley SE (2002) Essential role of MCM proteins in premeiotic DNA replication. *Mol Biol Cell* **13**:435–444.
 34. Liu Z, Li J, Chen J, Shan Q, Dai H, Xie H *et al* (2018) MCM family in HCC: MCM6 indicates adverse tumor features and poor outcomes and promotes S/G2 cell cycle progression. *BMC Cancer* **18**:200.
 35. Louis DN, Perry A, Reifenberger G, von Deimling A, Figarella-Branger D, Cavenee WK *et al* (2016) The 2016 World Health Organization Classification of Tumors of the Central Nervous System: a summary. *Acta Neuropathol* **131**:803–820.
 36. Markiewicz T, Grala B, Kozłowski W, Osowski S (2010) Computer system for cell counting in selected brain tumors at Ki-67 immunohistochemical staining. *Anal Quant Cytol Histol* **32**:323–332.
 37. Moncayo G, Grzmil M, Smirnova T, Zmarz P, Huber RM, Hynx D *et al* (2018) SYK inhibition blocks proliferation and migration of glioma cells and modifies the tumor microenvironment. *Neuro-Oncology* **20**:621–631.
 38. Ostrom QT, Gittleman H, Liao P, Vecchione-Koval T, Wolinsky Y, Kruchko C, Barnholtz-Sloan JS (2017) CBTRUS statistical report: primary brain and other central nervous system tumors diagnosed in the United States in 2010–2014. *Neuro-Oncology* **19**:v1–v88.
 39. Prayson RA, Castilla EA, Hembury TA, Liu W, Noga CM, Prok AL (2003) Interobserver variability in determining MIB-1 labeling indices in oligodendrogliomas. *Ann Diagn Pathol* **7**:9–13.
 40. Preusser M, Hoeflberger R, Woehrer A, Gelpi E, Kouwenhoven M, Kros JM *et al* (2012) Prognostic value of Ki67 index in anaplastic oligodendroglial tumours—a translational study of the European Organization for Research and Treatment of Cancer Brain Tumor Group. *Histopathology* **60**:885–894.
 41. Rosenberg S, Ducray F, Alentorn A, Dehais C, Elarouci N, Kamoun A *et al* (2018) Machine learning for better prognostic stratification and driver gene identification using somatic copy number variations in anaplastic oligodendroglioma. *Oncologist* **23**(12):1500–1510.
 42. Schrader C, Janssen D, Klapper W, Siebmann JU, Meusers P, Brittinger G *et al* (2005) Minichromosome maintenance protein 6, a proliferation marker superior to Ki-67 and independent predictor of survival in patients with mantle cell lymphoma. *Br J Cancer* **93**:939–945.
 43. Suzuki H, Aoki K, Chiba K, Sato Y, Shiozawa Y, Shiraishi Y *et al* (2015) Mutational landscape and clonal architecture in grade II and III gliomas. *Nat Genet* **47**:458–468.
 44. Uckun FM, Qazi S (2014) SYK as a new therapeutic target in B-cell precursor acute lymphoblastic leukemia. *J Cancer Ther* **5**:124–131.
 45. Van den Bent MJ, Brandes AA, Taphoorn MJB, Kros JM, Kouwenhoven MCM, Delattre JY *et al* (2013) Adjuvant procarbazine, lomustine, and vincristine chemotherapy in newly diagnosed anaplastic oligodendroglioma: long-term follow-up of EORTC brain tumor group study 26951. *J Clin Oncol* **31**:344–350.
 46. Van den Bent MJ, Carpentier AF, Brandes AA, Sanson M, Taphoorn MJB, Bernsen HJJA *et al* (2006) Adjuvant procarbazine, lomustine, and vincristine improves progression-free survival but not overall survival in newly diagnosed anaplastic oligodendrogliomas and oligoastrocytomas: a randomized European Organisation for Research and Treatment of Cancer phase III trial. *J Clin Oncol* **24**:2715–2722.
 47. Vigouroux C, Casse JM, Battaglia-Hsu SF, Brochin L, Luc A, Paris C *et al* (2015) Methyl(R217)HuR and MCM6 are inversely correlated and are prognostic markers in non small cell lung carcinoma. *Lung Cancer* **89**:189–196.
 48. Xu J, Zhang S, You C, Huang S, Cai B, Wang X (2007) Expression of human MCM6 and DNA Topo II alpha in craniopharyngiomas and its correlation with recurrence of the tumor. *J Neurooncol* **83**:183–189.
 49. Zeng A, Hu Q, Liu Y, Wang Z, Cui X, Li R *et al* (2015) IDH1/2 mutation status combined with Ki-67 labeling index defines distinct prognostic groups in glioma. *Oncotarget* **6**:30232–30238.

SUPPORTING INFORMATION

Additional supporting information may be found in the online version of this article at the publisher's web site:

Figure S1. *MCM6* and *MKI67* mRNA level distributions into two subgroups of higher (“-up”) and lower (“-down”) expressions. Transcriptomic samples (n = 68) are separated at the median expression for each gene and ordered according to their expression gradient for either *MCM6* or *MKI67*.

Figure S2. Correlations between immunohistochemistry (IHC) and mRNA level for Ki-67 (*MKI67*) and *MCM6*.

Figure S3. Correlation between mRNA expression levels of *MKI67* and *MCM6*.

Figure S4. Log₂-normalized gene expression levels for the upregulated pro-neural (A), epigenetic (B), and cell cycle (C) signatures, as well as the downregulated immune response (D), myelination (E) and glial cells differentiation (F) signatures for both *MCM6* and *MKI67* “-down” and “-up” samples (transcriptomics).

Figure S5. Significantly dysregulated KEGG pathways with an overall upregulation (Table as obtained with Gage) and map

of the cell cycle (GraphViz rendered with Pathview) in both *MCM6* (A) and *MKI67* (B) upregulated samples. Significantly (FDR < 0.01) down- and upregulated genes are colored from green to red, with respect to their fold change of expression (log2).

Figure S6. Survival analyses in grades II/III IDH-mutant/1p19q codeleted oligodendrogliomas selected from TCGA database. Kaplan–Meier curves with log-rank tests (overall survival). A. *MCM6* mRNA level, median threshold (arbitrary units). B. *MKI67* mRNA level, median threshold (arbitrary units). C. WHO 2016 grade.

Figure S7. K-means clustering based on *MCM6* and/or *MKI67* mRNA expression gradient (from lowest to highest) of the 35 transcriptomes of anaplastic IDH-mutant/1p19q codeleted oligodendrogliomas selected from TCGA bank. The K-means clustering delineated five significant clusters of co-expressed genes ($P < 0.05$) with highly correlated molecular functions. A. Heatmap of the 10 k-means clusters organized based on the extent of *MCM6* and *MKI67* expression (green, red and black indicate downregulated, upregulated and median genes, respectively). B. Overview of the most relevant functional annotations for the significantly over- and under-expressed clusters (in red and green hues, respectively, all $P(FDR) \leq 0.01$). Each of these clusters was compared to the clusters found of the POLA cohort, and their identities calculated based on the corresponding POLA clusters. C. Mean gene expression (overall with standard error at the mean) for each cluster where both upregulated samples for *MCM6* and/or *MKI67* are compared to their downregulated counterparts (AU—arbitrary units). Upregulated and downregulated samples are defined relatively to *MCM6* median gene expression.

Figure S8. K-means clustering based on *MCM6* and/or *MKI67* mRNA expression gradient (from lowest to highest) of the 98 transcriptomes of grades II and III IDH-mutant/1p19q codeleted oligodendrogliomas selected from TCGA bank. The K-means clustering delineated five significant clusters of co-expressed genes ($P < 0.05$) with highly correlated molecular functions. A. Heatmap of the ten k-means clusters organized based on the extent of *MCM6* and *MKI67* expression (green, red and black indicate downregulated, upregulated and median genes, respectively). B. Overview of the most relevant functional annotations for the significantly over- and under-expressed clusters (in red and green hues, respectively, all $P(FDR) \leq 0.01$). Each of these clusters was compared to the clusters found of the POLA cohort, and their identities calculated based on the corresponding POLA clusters. C. Mean gene expression (overall with standard error at the mean) for each cluster where both upregulated samples for *MCM6* and/or *MKI67* are compared to their downregulated counterparts (AU—arbitrary units). Upregulated and downregulated samples are defined relatively to *MCM6* median gene expression.

Table S1. K-means clustering from *MCM6* and *MKI67* expression gradients of 68 transcriptomes of anaplastic oligodendrogliomas from the POLA network. Functional annotations of

the genes present in the five significant groups of co-expressed genes ($P < 0.01$), sorted by gene ontology enrichment (FDR, false discovery rate; GO, gene ontology).

Table S2. Differential gene expression statistics (t-test) between *MCM6*-up and *MCM6*-down, and between *MKI67*-up and *MKI67*-down samples, sorted by P -value (BH, Benjamini–Hochberg; FDR, false discovery rate; GO, gene ontology; SD, standard deviation).

Table S3. K-means clustering from *MCM6* (or *MKI67*) expression gradients of 35 transcriptomes of grade III oligodendrogliomas from the TCGA bank. Functional annotations of the genes present in the five significant groups of co-expressed genes ($P < 0.01$), sorted by gene ontology enrichment (FDR, false discovery rate; GO, gene ontology).

Table S4. K-means clustering from *MCM6* expression gradients of 98 transcriptomes of grade II and grade III oligodendrogliomas from the TCGA bank. Functional annotations of the genes present in the six significant groups of co-expressed genes ($P < 0.01$), sorted by gene ontology enrichment (FDR, false discovery rate; GO, gene ontology).

APPENDIX

List of investigators

POLA Network: Amiens (Christine Desenclos, H. Sevestre), Angers (Philippe Menei, A. Rousseau), Annecy (T. Cruel, S. Lopez), Besançon (M.I. Mihai, A. Petit), Brest (R. Seizeur, I. Quintin-Roué), Bicêtre (C. Adam, F. Parker), Bordeaux (S. Eimer, H. Loiseau), Caen (L. Bekaert, F. Chapon), Clamart (D. Ricard), Clermont-Ferrand (C. Godfraind, T. Khallil), Clichy (D. Cazals-Hatem, T. Faillot), Colmar (C. Gaultier, M. C. Tortel), Cornebarrieu (I. Carpiuc, P. Richard), Créteil (W. Lahiani), Dijon (H. Aubriot-Lorton, F. Ghiringhelli), Lille (C-A. Maurage, E. Le Rhun), Limoges (E. M. Gueye, F. Labrousse), Lyon (F. Ducray, D. Meyronet), Marseille (O. Chinot), Montpellier (L. Bauchet, V. Rigau), Nancy (P. Beauchesne), Nantes (M. Campone, D. Loussouarn), Nice (D. Fontaine, F. Vandenbos-Burel), Nîmes (A. Le. Floch, P. Roger), Orléans (C. Blechet, M. Fesneau), Paris (A. Carpentier, A. Idbah, J. Y. Delattre [POLA Network National coordinator], K. Mokhtari, F. Bielle, S. Hamdi, M. Polivka), Poitiers (S. Milin), Reims (P. Colin, M. D. Diebold), Rennes (D. Chiforeanu, E. Vauleon), Rouen (O. Langlois, A. Laquerriere), Saint-Etienne (F. Forest, M. J. Motso-Fotso), Saint-Pierre de la Réunion (M. Andraud, G. Runavot), Strasbourg (B. Lhermitte, G. Noel), Suresnes (S. Gaillard, C. Villa), Toulon (N. Desse), Tours (C. Rousselot-Denis, I. Zemmoura), Toulouse (E. Cohen-Moyal, E. Uro-Coste), Villejuif (F. Dhermain).